NASA Technical Memorandum 87807

On Seasonal Variations of Mars' Gravitational Field

B. Fong Chao and David P. Rubincam

JANUARY 1987

NASA

NASA Technical Memorandum 87807

On Seasonal Variations of Mars' Gravitational Field

B. Fong Chao and David P. Rubincam
Goddard Space Flight Center
Greenbelt, Maryland

National Aeronautics
and Space Administration

**Scientific and Technical
Information Branch**

1987

ON SEASONAL VARIATIONS OF MARS' GRAVITATIONAL FIELD

INTRODUCTION

It is well-known that Mars has seasons like the Earth. However, the Mars' colder atmospheric temperature (in average some 70°K lower than the Earth's) and its predominantly carbon dioxide (CO_2) atmosphere (more than 95%) conspire to create a large exchange of CO_2 mass between the Martian atmosphere and polar caps. The mass exchange occurs in seasonal cycles: a great quantity of CO_2 condenses to form (or add to) the polar caps in winter and sublimes into the atmosphere in summer. The mass involved is at least 8×10^{15} kg, which is about 25% of the total mass of the Martian atmosphere, or equivalent to a cap of solid CO_2 extending to 45° latitude changing its thickness by some 20 cm (Hess et al., 1979). In contrast, the Earth's atmosphere only varies seasonally by about 1×10^{15} kg (or about 0.02% of the total), primarily due to variation of water vapor content (Trenberth, 1981).

The effect of this CO_2 mass redistribution on Mars' rotation has been discussed by Reasenberg and King (1979) and Cazenave and Balmino (1981). The present paper is an attempt to address quantitatively this CO_2-exchange effect on the Martian gravitational field. Qualitatively, the gravitational effect of any global-scale mass redistribution is largely decided by the ratio of the net redistributed mass to the total mass of the planet. For the Martian CO_2-exchange effect, the ratio is $8 \times 10^{15} / 6.4 \times 10^{23}$, or about 10^{-8}. No geological or geophysical phenomenon on Earth is known to produce a relative mass redistribution of nearly that size in a year. The post-glacial rebound of the mantle, the strongest southern oscillation / El Niño events in the atmosphere and the ocean, and the greatest earthquakes are all at least one to two orders of magnitudes smaller. Since even these geophysical phenomena are already being observed gravitationally by Earth-orbiting satellites (e.g., Rubincam, 1984; Gross and Chao, 1985), we can expect the CO_2-exchange effect on Mars to be detectable from future Mars orbiter missions. If so, the observed gravitational field changes can provide gross constraints on the meteorological models for Mars.

GENERAL FORMULATION

Let the coordinate system be such that the origin is at Mars' center of mass, and the x, y, and z axes define the 0°E Meridian, the 90°E Meridian, and the North Pole, respectively. We express the gravitational potential U of a planet at an external field point $\mathbf{r}_0$ through spherical harmonic expansion (e.g., Balmino, 1981):

$$U(\mathbf{r}_0) = \frac{GM}{r_0}\left[1 + \left(\frac{R}{r_0}\right)^2 C_{20}^{(H)}\, Y_{20}(\Omega_0)\right] + T(\mathbf{r}_0) \qquad (1)$$

where Ω is an abbreviation for the co-latitude θ and east longitude λ, $(r_0,\theta_0,\lambda_0) = (r_0,\Omega_0)$ is the spherical coordinate of $\mathbf{r}_0$, G is the gravitational constant, M the total mass, and R the mean radius of the planet. The spherical harmonics in this paper are defined as

$$Y_{lm}(\Omega) = [(2-\delta_{m0})(2l+1)(l-m)!/(l+m)!]^{1/2}\, P_{lm}(\cos\theta)\, e^{im\lambda} \qquad (2)$$

where l and m are respectively the degree and order, δ is the Kronecker delta function, P_{lm} is the associated Legendre function. We shall later use the index (l,m) to specify a particular harmonic component. The normalization in (2) is such that

$$\int Y_{l'm'}(\Omega)\, Y^*_{lm}(\Omega)\, d\Omega = 4\pi\,(2-\delta_{m0})\,\delta_{ll'}\,\delta_{mm'} \qquad (3)$$

where the asterisk denotes complex conjugation, $d\Omega$ is an element of solid angle, and the integration is over the unit sphere.

Neglecting higher order terms, the first two terms in equation (1) represent the potential the planet would have assumed in hydrostatic equilibrium (indicated by the superscript H) under rotation. That constitutes the reference spheroid. Thus the remaining term $T(\mathbf{r}_0)$ is the anomalous potential relative to the reference spheroid. It can be expressed as

$$T(\mathbf{r}_0) = \frac{GM}{r_0}\,\mathrm{Re}\left[\sum_{l=2}^{\infty}\sum_{m=0}^{l}\left(\frac{R}{r_0}\right)^l A_{lm}\, Y^*_{lm}(\Omega_0)\right] \qquad (4)$$

where Re denotes the real value. The normalization in (3) is chosen such that the harmonic coefficient A_{lm} in (4), here referred to as the complex Stokes coefficient, is directly related to the ordinary (normalized) Stokes coefficients C_{lm} and S_{lm} (c.f. Kaula, 1966) simply through

$$A_{lm} = C_{lm} + iS_{lm}. \qquad (5)$$

The geoid of a planet is the equipotential surface on which $T(\mathbf{r}_0)=0$. Its departure from the reference spheroid is the geoid height (c.f. Figure 3).

By comparing equations (1) and (4) with the multipole expansion of U, one can relate the complex Stokes coefficients to the density distribution $\rho(\mathbf{r})$ of the planet (e.g., Chao & Gross, 1986):

$$A_{lm} = \frac{1}{(2l+1)\ MR^l} \int \rho(\mathbf{r})\ r^l\ Y_{lm}(\Omega)\ dV \tag{6}$$

where dV is the volume element, and the integration is over the entire volume V of the planet.

Now suppose a time-varying change $\Delta\rho(\mathbf{r},t)$ is imposed upon $\rho(\mathbf{r})$. In an Eulerian description, the resultant change in the complex Stokes coefficient follows immediately from equation (6):

$$\Delta A_{lm} = \frac{1}{(2l+1)\ MR^l} \int \Delta\rho(\mathbf{r})\ r^l\ Y_{lm}(\Omega)\ dV \tag{7}$$

where the integration is now over the changing volume of the planet. In the following we shall translate these changes into equivalent changes in the geoid height N using Bruns formula N=T/g, where $g = GM/R^2$ is the surface gravitational acceleration (e.g., Rapp, 1975). This, in the present case, gives the root-mean-square (rms) amplitude of the (l,m) component of the geoid height change:

$$\Delta N_{lm}(t) = R\ |\ \Delta A_{lm}(t)\ |. \tag{8}$$

$\Delta N_{lm}(t)$ (in millimeters) provides a comfortable measure of the effect of $\Delta\rho(\mathbf{r},t)$ on the geoid.

CO_2 MASS EXCHANGE ON MARS

Equation (7) will now be applied to the CO_2 mass exchange between the atmosphere and polar caps on Mars. First, we notice that this mass exchange occurs in a thin veneer on the Martian surface (only a few tens of kilometers thick), and any radial movement is negligible in the presence of the global-scale lateral movement. Therefore, to a good approximation we can take r=R and use surface density $\Delta\sigma(\Omega,t)$ in place of the volume density $\Delta\rho(r,t)$. Equation (7) then reduces to

$$\Delta A_{lm}(t) = \frac{R^2}{(2l+1)M} \int \Delta\sigma(\Omega,t)\, Y_{lm}(\Omega)\, d\Omega \qquad (9)$$

where the integration is over the entire surface of the planet.

The simplicity of equation (9) is deceiving because to obtain the true $\Delta\sigma(\Omega,t)$ one should in general take into consideration the gravitational interaction between the shifting mass and the rest of the planet, or, in the present case, the effect of the elastic yielding of the solid Mars due to the loading and unloading of the CO_2 mass. However, as shown below, this interaction is small on Mars so that the solid Mars can be treated as a rigid body.

The relevant parameter is the load Love number k_l' of degree l and how it compares to unity. Assuming a homogeneous planet,

$$k_2' = \frac{-1}{1 + (19\bar{\mu} / 2\bar{\rho}gR)} \qquad (10)$$

(Munk & MacDonald, 1960). Here $\bar{\rho}$ and $\bar{\mu}$ are the average density and rigidity, respectively, and $\bar{\rho} = 3.9 \times 10^3$ kg m^{-3}. If we assume that Mars has the same average rigidity as the Earth, $\bar{\mu} \simeq 1.45 \times 10^{11}$ kg m^{-1} s^{-1}, then $|k_2'| = 0.037$, or about one eighth of the Earth's (Lambeck, 1980). This, in fact, may be an upper limit on $|k_2'|$ since Mars, being a colder planet internally, might have a higher rigidity than the Earth's. Likewise the other $|k_l'| \ll 1$. We thus conclude that the elastic yielding of the solid Mars can be safely neglected. We shall also neglect the self-gravitation within the CO_2 mass itself. The resultant errors are relatively small compared with those introduced by the simplifications we shall make in our model below. In the rigid solid Mars approximation, we can extend equation (9) to encompass l=1 (m=0,±1) terms. These terms simply give the relative shift in the center of mass of the solid part of Mars due to the CO_2 variations.

Now let us follow the seasonal journey of the CO_2 mass and examine separately the contributions to (9) of two phases: (i) the waxing and waning of the solid CO_2 in polar caps, and (ii) the geographical distribution of the gaseous CO_2 in the atmosphere. The two phenomena, of course, accompany each other inasmuch as the total CO_2 mass is constant. The total CO_2-exchange effect is simply the sum of the two contributions.

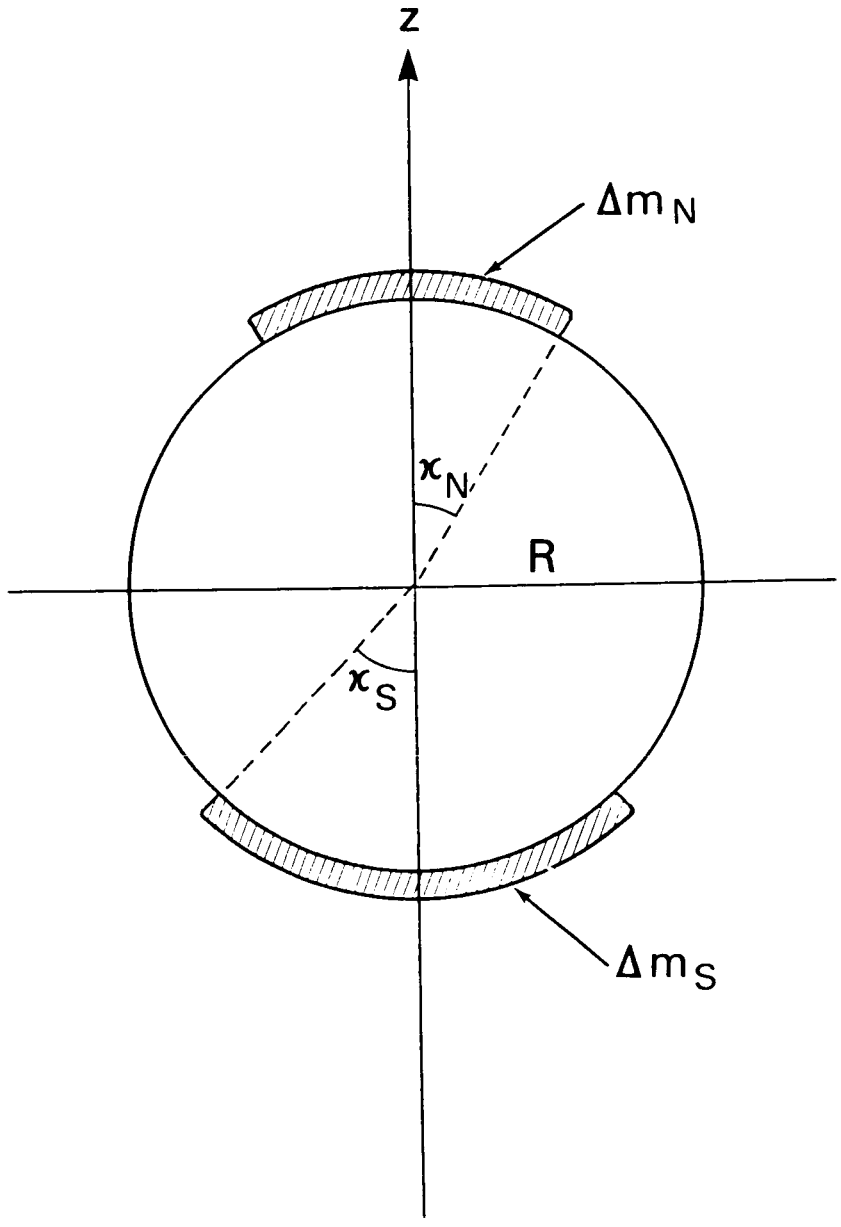

Fig. 1. A cross section of Mars showing schematically two solid CO_2 polar caps.

Waxing and Waning of Polar Caps

First let us examine the simple geometry where the seasonal condensation and sublimation occur uniformly over the polar caps, and the caps are circular and symmetrical with respect to the poles (Figure 1). The surface density $\Delta\sigma(\Omega,t) = \Delta\sigma(t)$ is thus a constant of position on the caps which extend to a constant angle κ from the poles.

For $m\neq 0$, equation (9) gives $\Delta A_{lm} = 0$, an expected result in light of the axial symmetry under the present assumptions. For $m=0$, after some simple algebra, equation (9) leads to

$$\Delta A_{l0}(t) = \Delta C_{l0}(t)$$

$$= \left[\frac{1}{\sqrt{2l+1}\ (1-\cos\kappa)} \int_{\cos\kappa}^{1} P_l(\mu)\ d\mu\ \frac{\Delta M(t)}{M} \right]_n + (-1)^l \left[\text{same} \right]_s \qquad (11)$$

where P_l is the Legendre function of degree l, $\Delta M(t) = 2\pi R^2(1-\cos\kappa)\Delta\sigma(t)$ is the total CO_2 mass accumulated on the cap at any given moment, and the subscripts n and s indicate the northern and southern hemispheres, respectively. Due to the eccentricity of the Mars' orbit the southern CO_2 polar cap is considerably more massive and extensive than its northern counterpart (Hess et al., 1979). At the peak of its formation, the angular extent κ_s actually varies with longitude between 40° and 50°, according to Viking orbiter observations (Briggs et al., 1977). For simplicity we shall take as an average $\kappa_s=45°$. The value of κ_n is less certain. The variation of the CO_2 mass in the polar caps, $\Delta M(t)$, can be estimated from the atmospheric pressure recordings of the two Viking landers (Hess et al., 1979, 1980). It is shown schematically in Figure 2, where the zero level corresponds to the minimum polar cap CO_2 (or, equivalently, maximum atmospheric CO_2). Here an annual period (669 sols, or 687 Earth days) and a semi-annual period dominate. Although it is not possible from these records to separate the contributions from the northern and southern caps, each cap is responsible for essentially half a (Martian) year. It is interesting to note from equation (11) that the variation in the Stokes coefficient, ΔC_{l0}, will follow the sum of the contributions from both caps if l is even, and the difference if l is odd. Thus, under the present simplification, if we can observe two varying $C_{l0}(t)$, one for an even l and one for an odd l, it is in principle possible to solve for $\Delta M_n(t)$ and $\Delta M_s(t)$ using equation (11), thus providing two important constraints on meteorological models for Mars.

It is also evident from equation (11) that the amplitude becomes progressively smaller as l increases. Here we shall only consider a few lowest degree terms by evaluating their maximum amplitudes which occur at the peak of formation of the southern cap ($t=t_0$, see Figure 2). Thus, substituting into equation (11) the value for ΔM, $\Delta M_s(t_0) = 8 \times 10^{15}$ kg, and $\kappa_s=45°$, we get $\Delta C_{l0}(t_0)$ for $l=1$-5, listed in Table 1. Table 1 also shows the corresponding amplitude of change in the more familiar zonal J_l coefficients which are related to C_{l0} by $J_l = -\sqrt{(2l+1)}C_{l0}$, as well as the rms amplitude

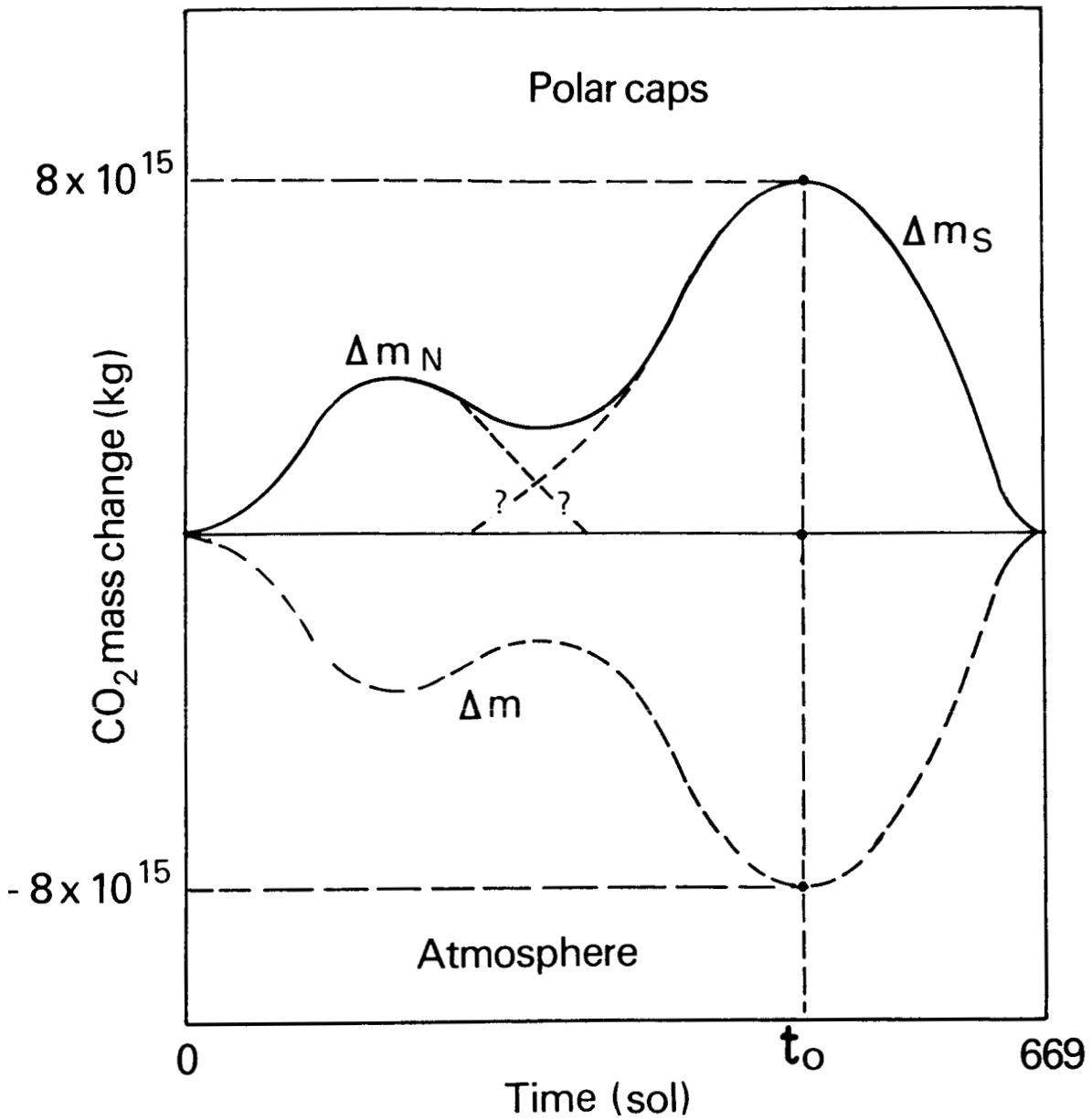

Fig. 2. CO_2 mass change in the course of one Martian year where the zero time (t=0) corresponds to the winter solstice (adopted from Hess et al., 1980). The upper curve represents the formation of the solid CO_2 polar caps, and the lower curve represents the corresponding loss of atmospheric CO_2.

in the corresponding geoid height change as given by equation (5) using R=3390 km. The largest change is in the l=1 term, which corresponds to a maximum shift of $\sqrt{(2l+1)}\Delta N_{10}$ = 36 mm by the solid planet with respect to the center of mass at $t=t_0$. The yearly peak-to-peak variation taking into account both northern and southern caps is about 52 mm. The most geodetically interesting change, however, is in J_2 which is the second largest term: $\Delta J_2 = -7.5 \times 10^{-9}$. The nominal value of J_2 has been well determined (e.g., Reasenberg et al., 1975) to be $J_2 = 1.956 \times 10^{-3}$. The maximum amplitude of the relative seasonal change is therefore $\Delta J_2/J_2$ = 3.8 ppm (parts per million). In comparison, this is two orders of magnitude larger than the observed secular change in the Earth's J_2 (presumably due to the post-glacial rebound of the mantle) which is found to be only 0.024 ppm per year (Rubincam, 1984).

The values in Table 1 are obtained under the simplification of a uniform condensation/sublimation of solid CO_2 over the entire polar caps (Figure 2). The real distribution, however, is probably more concentrated toward the pole. The latter will yield somewhat larger changes in $C_{10}(t)$. Hence Table 1 is only a lower bound on $\Delta C_{10}(t_0)$. For example, the extreme case where all the condensed CO_2 is concentrated at the pole ($\kappa \to 0$) gives, according to equation (11), a $\Delta J_2(t_0)$ of -12.5×10^{-9} which is some 60% larger than the uniform case. A more realistic, "layered cake" model where the CO_2 layer between $\kappa=0°$ and 22.5° is twice as thick as that between $\kappa=22.5°$ and 45° yields a $\Delta J_2(t_0)$ of -8.7×10^{-9}.

Table 1. Maximum gravitational effect of the changing polar cap CO_2 (equation 11).

l	ΔC_{10} ($\times 10^9$)	ΔJ_l ($\times 10^9$)	ΔN_{10} (mm)
1	-6.1	10.6	21
2	3.4	−7.5	11
3	-1.5	4.0	5.0
4	0.31	-0.94	1.1
5	0.30	-1.0	1.0

Geographical Distribution of the Atmosphere

The Martian surface topography will influence the way the changing atmospheric CO_2 mass distributes itself geographically; that, in turn, will produce changes in the gravitational field. For simplicity, we here assume that the atmosphere is always in hydrostatic equilibrium. Physically, this requires an instantaneous redistribution of CO_2 mass over the globe. This is permissible since we are only concerned with seasonal periods which are much longer than the time scale for Martian atmospheric circulation.

In equilibrium, any isopycnic (constant density) surface of the atmosphere will follow an equipotential surface of the gravitational field. In a hypothetical case where the surface topography is itself a geoid (for example, if the entire planet were covered by an ocean), the geographic distribution of the atmosphere would be practically uniform in the sense that its surface density $\sigma(\Omega,t)$ would be independent of geographic location Ω, changing only with time t. In such a case, the changing atmosphere has no gravitational effect (except on the total mass which, of course, is compensated by the waxing and waning of polar caps). In reality, the Martian surface topography is not a geoid. In fact, Mars, unlike the Earth, has a relatively large surface relief, so much so that a substantial fraction of the atmosphere can "feel" the topography. The atmospheric surface density σ will be smaller where the topography protrudes the geoid (e.g. over a high plateau), and larger otherwise (e.g. over a low basin).

Thus, it is the departure of the true topography from the geoid that determines how $\sigma(\Omega)$ is to deviate from being uniform. This "effective topography", denoted by $h(\Omega)$ (see Figure 3), can be written in terms of spherical harmonics as

$$h(\Omega) = R\ \mathrm{Re}\left[\sum_{l=1}^{\infty} \sum_{m=0}^{l} H_{lm}\, Y_{lm}^{*}(\Omega) \right]. \qquad (12)$$

The coefficient H_{lm}, using equation (4) and Bruns formula, is

$$H_{lm} = H'_{lm} - A_{lm} \qquad (13)$$

where H'_{lm} is the complex harmonic coefficient of the true topography $h'(\Omega)$ (relative to the reference spheroid):

$$h'(\Omega) = R\ \mathrm{Re}\left[\sum_{l=1}^{\infty} \sum_{m=0}^{l} H'_{lm}\, Y_{lm}^{*}(\Omega) \right] \qquad (14)$$

Notice that in equations (12) and (14) we included first-degree (l=1) harmonics. They represent a displacement of the center of figure from the center of mass (Bills and Ferrari, 1978).

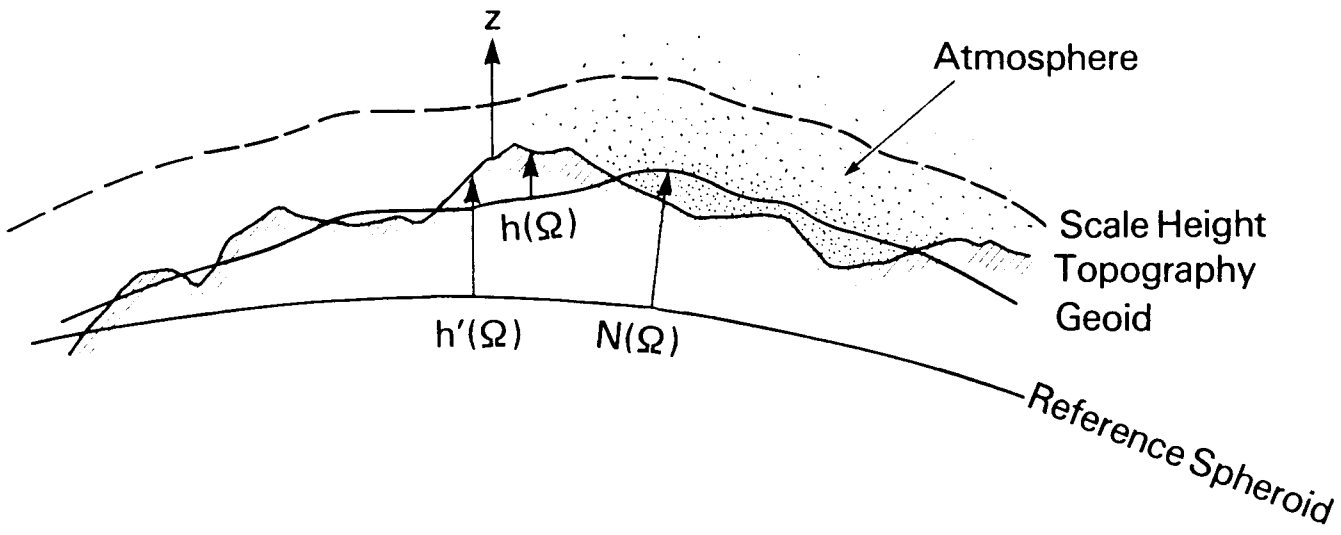

Fig. 3. Schematic diagram showing the distribution of atmosphere as specified by the scale height, in relation to the topography, the geoid, and the reference spheroid. N: geoid height, h': true topography, h: effective topography, z: vertical height from surface.

Table 2. Maximum gravitational effect of the changing atmospheric CO_2 (equation 20).

(l,m)	$(\Delta C_{lm}, \Delta S_{lm})$ $(\times 10^9)$	ΔJ_l $(\times 10^9)$	ΔN_{lm} (mm)
(1,0)	(-0.48 --)	0.84	1.6
(1,1)	(-0.021 0.51)	--	1.7
(2.0)	(-0.73 --)	1.6	2.5
(2,1)	(0.11 -0.16)	--	0.67
(2,2)	(-0.31 -0.25)	--	1.4
(3,0)	(0.046 --)	-0.12	0.16
(3,3)	(0.085 -0.25)	--	0.88

From $h(\Omega)$ we can obtain $\Delta\sigma(\Omega)$ for the atmospheric CO_2 as follows. The lower atmosphere is where virtually all the atmospheric mass resides. The equilibrium density variation there can be approximated by the isothermal profile

$$\rho(z,\Omega) = \rho_0 \exp[-(z+h(\Omega))/Z] \tag{15}$$

where z is the vertical height from the surface, and ρ_0 is the atmospheric density on the geoid $z=-h(\Omega)$. Z is the atmospheric scale height (see Figure 3) and is given by

$$Z = kT/\nu g \tag{16}$$

where k is the Boltzmann constant (1.38×10^{-23} J $^\circ K^{-1}$), T is the temperature of the lower atmosphere, ν is the molecular weight of CO_2 (7.3×10^{-26} kg), and the surface gravity $g=3.7$ m s^{-2}.

The temperature T, and hence the scale height Z are of course functions of time and position. For simplicity we shall take T to be the spatially averaged atmospheric temperature over the globe at any given time. By doing so we are essentially disregarding the effect on Z due to diurnal fluctuations in the temperature. This is permissible because these fluctuations average out on a seasonal time scale and has little bearing in the present study. However, T is still a function of the time of the year because of the eccentricity of the Mars' orbit relative to the Sun. In particular, T will be highest near perihelion (late southern spring) and lowest near aphelion (late southern fall). A brief examination of Figure 2 reveals that at the times under consideration, namely the times when the amount of the atmosphere is at its maximum ($t=0$) and minimum ($t=t_0$), the globally averaged T should be about the same and somewhat higher than the yearly mean value. Therefore we can take T as a constant for which our best judgment is $\bar{T}$ = 220°K, corresponding to a nominal Z = 11 km according to equation (16). For Viking lander observations during landing at Northern mid-latitudes in summer, the reader is referred to Seiff and Kirk, 1977. We should mention that we have considered the surface values only. In reality, the temperature decreases with increasing altitude fairly rapidly, so that the "effective" scale height is somewhat smaller than 11 km. In other words, 11 km is probably an upper bound on Z.

Under all the simplifications made so far, the change in surface density of the atmospheric CO_2 is

$$\Delta\sigma(\Omega,t) = \int_0^\infty \Delta\rho(z,\Omega,t)\, dz = \Delta\rho_0(t)\, Z \exp[-h(\Omega)/Z] \ . \tag{17}$$

To proceed, we notice that, although the true Martian topography (h') is at places comparable to or even exceeds the atmospheric scale height Z, the effective topography (h) is generally much smaller. In fact, the rms amplitudes $R|H_{lm}|$ of the individual (l,m) harmonic component of h are all small compared with Z (the largest term is only about 0.1Z, see Bills and Ferrari, 1978). This is a consequence of the high correlation between the topography and the gravitational field of Mars (e.g., Bills & Ferrari, 1978), especia-

lly in low-degree harmonics on which we shall concentrate. Therefore we can approximate $\exp[-h(\Omega)/Z]$ by substituting the expression (12) for $h(\Omega)$ and retaining the first-order terms in a Taylor expansion

$$\exp[-h(\Omega)/Z] = 1 - \frac{R}{Z}\,\mathrm{Re}\left[\sum_{l=1}^{\infty}\sum_{m=0}^{l} H_{lm}\, Y^{*}_{lm}(\Omega)\right] \qquad (18)$$

Substituting this expression into equation (17) and then into (9) leads to

$$\Delta A_{lm}(t) = \frac{\Delta M(t)}{4\pi(2l+1)M}\int\left[1 - \frac{R}{Z}\,\mathrm{Re}\left[\sum_{l'=1}^{\infty}\sum_{m'=0}^{l'} H_{l'm'}\, Y_{l'm'}(\Omega)\right]\right] Y_{lm}(\Omega)\, d\Omega \qquad (19)$$

where $\Delta M(t) = 4\pi R^2 Z \Delta\rho_0(t)$ is the total CO_2 mass added to the atmosphere. Using the orthogonality (3) of the spherical harmonics, equation (19) reduces to

$$\Delta A_{lm}(t) = -\frac{2-\delta_{m0}}{2l+1}\,\frac{RH_{lm}}{Z}\,\frac{\Delta M(t)}{M} \qquad (20)$$

as long as $l,m \neq 0$. Equation (20) is the final formula for the gravitational effect due to the changing atmospheric CO_2 mass. Note that this effect separates naturally into spherical harmonics, in the sense that the (l,m) component of the change in the complex Stokes coefficient, ΔA_{lm}, is directly and solely proportional to the (l,m) component of the effective topography, RH_{lm}. This further justifies a posteriori the approximation in equation (18). The atmospheric CO_2 mass change $\Delta M(t) = -[\Delta M_n(t) + \Delta M_s(t)]$ is shown in Figure 2. The H_{lm} coefficients can be obtained, according to equation (13), from the H_{lm} estimates published by Bills and Ferrari (1978) and the A_{lm} estimates by Christensen and Balmino (1979) and Balmino et al. (1982). Note that the S_{lm} values in these studies should change sign to conform to our present definition of the (east) longitude λ.

Table 2 presents the maximum amplitude of $\Delta A_{lm}(t)$, which occurs at $t=t_0$ when $\Delta M(t_0) = -8 \times 10^{15}$ kg (Figure 2), for some most prominent low-degree harmonics:

The first-degree ($l=1$) harmonics gives the change in the relative displacement of the center of figure from the center of mass (Bills and Ferrari, 1978). This displacement is found to be 2.4 mm in the direction (92°E, 44°N) using our longitude convention.

The change in the (2,0) harmonic, and hence in J_2, is again the largest term, this time reflecting the solid Mars' large deviation from a hydrostatic equilibrium state. It is out of phase with the polar cap contribution, decreasing the amplitude by nearly one quarter. The reason these two changes in J_2 are out of phase is due to Mars' excess topographic oblate-

ness. The polar regions are topographically low. Hence the excess atmosphere there decreases when the caps grow, increasing J_2. Note that the change in the (3,0) harmonic, and hence in J_3, is also out of phase with respect to the polar cap contribution, but its amplitude is negligible.

The change in the (2,1) harmonics gives rise to a shift in the principal axis of the greatest moment of inertia, or the figure axis. The angular departure of the figure axis from the z axis is usually expressed in terms of its x- and y-components, $\Psi = \Psi_x + i\Psi_y$. This function Ψ excites the polar motion and is thus known as the polar-motion excitation function (Munk and MacDonald, 1960). For any excitation mechanism that loads the planet (such as atmospheric variations), Ψ can be found by

$$\Psi(t) = - \sqrt{5} \, [\, \Delta C_{21}(t) + i \Delta S_{21}(t) \,] \, / \, (\sqrt{3} \, J_2). \qquad (21)$$

The excitation function in the present case has some interesting features, as can be shown from equation (21) and Table 2. First, it stays strictly along a fixed meridian (125°E), simply because the topography is fixed. Second, its maximum amplitude is 26 milliarcsecond (mas), equivalent to a surface polar displacement as large as 45 cm. Compare this with that on Earth produced by the great 1960 Chilean earthquake, 23 mas (e.g., Chao & Gross, 1986) or the strong El Nino event of 1982-1983, ~40 mas (Gross and Chao, 1985). Unfortunately this rather strong excitation, at annual (669 sols) and semi-annual periods, is not likely to generate a large polar motion. This is because Mars, assuming an Earth-like rigidity, has a free wobble period of about 200 sols. Hence, unlike the Earth, no resonance should be expected from seasonal excitations.

The (2,2) and (3,3) harmonics are the only other components that have geoid height changes comparable to the above changes. They are exceptionally large on Mars simply because of the existence of the extensive Tharsis construct and its antipodal, but smaller, uplift.

Discussion

The variations in Mars' gravitational field due to the CO_2 mass exchange are generally very large compared with their terrestrial counterparts. Nevertheless, whether they can be observed by the upcoming MOM (Mars Observer Mission, due to be launched in 1990) is presently uncertain. A simple simulation made by F. Lerch and C. Wagner for an MOM proposal (1985) has indicated that, using Doppler tracking data of the MO orbit alone, the change in J_2 can be marginally detected. If in addition the surface altimetry data (as differences at crossovers) are available, then the accuracy in the gravitational field determination is expected to be improved. It may then be possible to detect changes in J_2 to a higher precision, thus placing constraints on the meteorological models of Mars. However, the simulation is done under the assumption that all favorable conditions prevail throughout the MOM lifetime (1 Martian year), and that no non-gravitational forces is acting on the spacecraft. The latter includes the atmospheric drag whose effect on the MO orbit, according to some estimates, may completely obscure the orbital effects caused by the small seasonal variations in the gravitational field. At the present time, simply too little about the Martian atmospheric density is known to warrant any further modeling.

References

Balmino, G., 1981. Gravity field and rotation of planets: A review from the point of view of planetary geodesy. Ann. Geophys., 37, 161-172.

Balmino, G., B. Moynot, and N. Vales, 1982. Gravity field model of Mars in spherical harmonics up to degree and order eighteen. J. Geophys. Res., 87, 9735-9746.

Bills, B.G., and A.J. Ferrari, 1978. Mars topography harmonics and geophysical implications. J. Geophys. Res., 83, 3497-3508.

Briggs, G.A., K. Klaasen, T. Thorpe, J. Wellman, and W. Baum, 1977. Martian dynamical phenomena during June-November 1976 Viking orbiter imaging results. J. Geophys. Res., 82, 4121-4149.

Cazenave, A., and G. Balmino, 1981. Meteorological effects on the seasonal variations of the rotation of Mars. Geophys. Res. Lett., 8, 245-248.

Chao, B.F., and R.S. Gross, 1986. Changes in the Earth's rotation and low-degree gravitational field induced by earthquakes, submitted to Geophys. J. Roy. Astron. Soc.

Christensen, E.J., and G. Balmino, 1979. Development and analysis of a twelfth degree and order gravity model for Mars. J. Geophys. Res., 84, 7943-7953.

Davies, D.W., C.B. Farmer, and D.D. LaPorte, 1977. Behavior of volatiles in Mars' polar areas: A model incorporating new experimental data. J. Geophys. Res., 82, 3815-3822.

Gross, R.S., and B.F. Chao, 1985. Excitation study of the LAGEOS-derived Chandler wobble. J. Geophys. Res., 90, 9369-9380.

Hess, S.L., R.M. Henry, and J.E. Tillman, 1979. The seasonal variation of atmospheric pressure on Mars as affected by the south polar cap. J. Geophys. Res., 84, 2923-2927.

Hess, S.L., J.A. Ryan, J.E. Tillman, R.M. Henry, and C.B. Leovy, 1980. The annual cycle of pressure on Mars measured by Viking landers 1 and 2. Geophys. Res. Lett., 7, 197-200.

Kaula, W.M., 1966. Theory of Satellite Geodesy. Blaisdell , Waltham, Mass.

Lambeck, K., 1980. The Earth's Variable Rotation. Cambridge Univ. Press, New York.

Munk, W.H., and G.J.F. MacDonald, 1960. The Rotation of the Earth. Cambridge Univ. Press, New York.

Rapp, R.H., 1975. The Earth's gravity field. Geophys. Surveys, 2, 193-216.

Reasenberg, R.D., I.I. Shapiro, and R.D. White, 1975. The gravity field of Mars. Geophys. Res. Lett., 2, 89-92.

Reasenberg, R.D., and R.W. King, 1979. The rotation of Mars. J. Geophys. Res., 84, 6231-6240.

Rubincam, D.P., 1984. Postglacial rebound observed by LAGEOS and the effective viscosity of the lower mantle. J. Geophys. Res., 89, 1077-1087.

Seiff, A., and D.B. Kirk, 1977. Structure of the atmosphere of Mars in summer at mid-latitudes. J. Geophys. Res., 82, 4364-4378.

Trenberth, K.E., 1981. Seasonal variations in global sea level pressure and the total mass of the atmosphere. J. Geophys. Res., 86, 5238-5246.

BIBLIOGRAPHIC DATA SHEET

1. Report No.	2. Government Accession No.	3. Recipient's Catalog No.
NASA TM-87807		

4. Title and Subtitle	5. Report Date
On Seasonal Variations of Mars' Gravitational Field	January 1987
	6. Performing Organization Code: Code 621

7. Author(s)	8. Performing Organization Report No.
B. Fong Chao and David P. Rubincam	87B0134

9. Performing Organization Name and Address	10. Work Unit No.
Geodynamics Branch Laboratory for Terrestrial Physics Goddard Space Flight Center Greenbelt, MD 20771	11. Contract or Grant No.
	13. Type of Report and Period Covered: Technical Memorandum
12. Sponsoring Agency Name and Address National Aeronautics and Space Administration Washington, DC 20546	14. Sponsoring Agency Code

15. Supplementary Notes

16. Abstract

A great quantity of CO_2 is exchanged between the Martian atmosphere and polar caps in the course of a Martian year. This exchange occurs in seasonal cycles: CO_2 condenses to form the polar caps in winter and sublimes into the atmosphere in summer. The mass involved is about 25% of the total mass of the Martian atmosphere. This paper studies the effects of the CO_2 mass redistribution on the Mars' gravitational field. Two mechanisms are examined: (i) the waxing and waning of solid CO_2 in the polar caps, and (ii) the geographical distribution of gaseous CO_2 in the atmosphere. The maximum changes produced by (i) in the low-degree zonal J_ℓ harmonics in the Mars' gravitational field are found to be as much as 7.5×10^{-9} for J_2 (corresponding to 1.1 cm change in the geoid), and about half as much for J_3. The effect of (ii) on some most prominent low-degree harmonics (for $\ell=1$-3) in the "effective topography" (defined as the departure of the true topography from the geoid) is also evaluated. Their magnitudes are large by Earth standards. Whether they can be observed by the upcoming Mars Observer is presently uncertain.

17. Key Words (Selected by Author(s))	18. Distribution Statement
Mars gravity Seasonal variation CO_2 Polar Caps	Unclassified - Unlimited Subject Category 91

19. Security Classif. (of this report)	20. Security Classif. (of this page)	21. No. of Pages	22. Price*
Unclassified	Unclassified	20	A02

*For sale by the National Technical Information Service, Springfield, Virginia 22161.

NASA-Langley, 1987